

Small island morphometry analysis with remote sensing and GIS methods on the Satonda volcanic island

Triyono^{1,*}, Salvienty Makarim², and Surahman³

¹ Marine Research Center, Ministry of Marine Affairs and Fisheries, Jakarta, Indonesia

² Marine Research Center, Ministry of Marine Affairs and Fisheries, Jakarta, Indonesia

³ Hydro-Oceanography Center, Indonesian Navy, Jakarta, Indonesia

Abstract: DEMNAS and Sentinel-1 are profoundly utilized for the small island morphometry analysis. This study explores the Satonda Island-West Nusa Tenggara landforms through the morphometry analysis using the DEM application and GIS analysis. As a volcanic island the Satonda Island coverage area is approximately about 2.600- hectare dominated by the slopes with the steep slope ($16^{\circ} - 35^{\circ}$) at the northwest in a moderately steep ($8^{\circ} - 16^{\circ}$) at the southeast. Here, we uncover that the Satonda Island experiences five landforms carved by volcanic processes and other five are generated by the marine processes. As a typical of volcanic island, this island has a cone shape with the caldera founded in the middle with the radial flow pattern.

1 Introduction

The main volcanic landforms in Indonesia are dominated by stratovolcano cones, calderas, and tectonic volcanic depressions with tuff ignimbrite plateaus. Volcanism in Indonesia is related to the location of major plate tectonic subduction zones and their origin and nature are like those in the Circum-Pacific volcanic belt. The Indo-Australian (Indian Ocean) plate plays an important role in southern Indonesia (Sumatra, Java, Nusa Tenggara islands) while the Pacific Ocean plate, including the Philippine plate plays a similar role in northeastern Indonesia [1]

Indonesian tropical climate is a matter in the development of volcanic slopes although the upper slopes of stratovolcanoes are generally dominated by gravitational forces on volcanic debris so that the slope angle has a maximum critical angle (angle of repose). On the lower slopes the development is influenced by the rain that infiltrates lava causing "wet" transportation so that the slope gradient is 8° - 12° [2]. There are 85% of pyroclastic cones having an elliptical shape with a ratio of 1:2 or 4:5 between the minimum and maximum cone base shaft length [3].

The classification of volcano typology is important as a basis for knowledge of risk assessment and disaster mitigation. Grouping is done by evaluating geomorphological

* Corresponding author: triyonodkp2@gmail.com

conditions and geological aspects [2]. Surface roughness is the key to understand soil and landscape properties in micrometeorology, agricultural hydrology, and volcanology, as well as other earth sciences. In terms of analyzing surface roughness, close-range stereophotogrammetry techniques can be used by extracting a Digital Terrain Model (DTM) [5,6]. Surface roughness is a measure of surface texture that is quantified by the vertical deviation of the surface from its ideal shape. If the deviation is high, the surface is rough, if it is low, the surface is smooth [7]. The most common and easiest to use roughness parameter is the root-mean-square (RMS) deviation or standard deviation of the average height [8], [2,7].

Volcano morphometry can be used in the accurate measurement of eruption models based on the morphology of the volcano body and allows to calculate the volume of erupted material as well as other formations such as slopes and terrain orientation after eruption [9]. Morphometric data determines whether the volcanic formation is aggrading or degrading. This study aims to describe and quantify the morphometric parameters of the volcano using GIS morphometric analysis.

Morphological parameters and their derivatives can be determined more accurately than using previous methods [9]. Satonda volcano emerges from the surface of the seafloor as a deformed cone and forms a caldera. In morphometric calculations, the volcano cone was measured using DTM calculations at high resolution (5x5m pixels) for a scale of 1:5,000, with necessary smoothing and using a mean differential geometry approach [11]. To obtain the calculation of morphometric parameters and to be able to adjust the appropriate resolution, the data used is a DEM obtained from the extraction of Maxar satellite images on Google Earth. Since 2005, Google Earth has used SRTM data as baseline elevation data to provide high-resolution elevation data with elevation accuracy of about 1.85 m RMSE, but still meets spatial requirements for large areas, urban planning, and classification maps [12].

The volcano classification based on morphometry is mostly applied for the volcanoes on land aiming for the importance of volcanic hazard/disaster mitigation. Meanwhile the disaster mitigation from submarine volcano is still less implementation when the disaster is more high risk than the land volcano. It is because of the eruption disaster from the submarine volcano can also generate the high wave on the sea. Through the volcano classification based on the morphometry analysis, the figure of volume and characteristic volcanoes can be achieved. The difficulties to identify the morphometry of submarine volcano is the lack of available bathymetry data on the foot of submarine volcano.

The Satonda Island is a volcanic island with a caldera in its crater. Volcanic islands are characterized by radial centrifugal river flow patterns [10]. According to Warren [1], caldera peaks are common formations formed during Plinian eruptions in the past. Calderas produced by the discharge of very large amounts of basaltic lava do not occur in Indonesia.

2 Material and methods

The bathymetry data used was the result of field measurements with a Single Beam Echosounder (SBES) on April 02-12, 2023. To create a 3D view, the DEM is composed of a series of grid points showing elevation values as a triangulated irregular network (TIN) where each point has coordinates and the surface represents a triangular plane [11]. Geomorphological analysis includes measurements of average slope, mean radius, and surface roughness, then combined with geological aspects and rainfall rate [2]. In this study, rainfall was not considered because the research object was a single object. Geological conditions were considered based on map data and previous research. In addition, geological conditions can be reflected by the drainage pattern. The 3D calculation of the surface base is

calculated from the outline with the inverse distance weighting (IDW) technique and then used to estimate the height and volume [4]. DEM accuracy is obtained through calculations with the approaches: (1). comparing elevations from contour lines and interpolated DEM values, (2). comparing 3D object volume calculations, and (3). comparing 3D object slope estimates classifications [2]. This study provides bathymetry data and the surface land elevation data that are processed serving as a Digital Elevation Model (DEM). Subsequently from the DEM data, the hill slope measurement is utilized and then it is portrayed into 2D shape. Slope class is defined with natural break methods, one of slope classification technique in GIS (Table 1).

Table 1. Slope and radius classification

Slope classification	Slope (°)	Radius Classification	Radius (km)
Very gentle	< 5°	Small	< 5 km
Gentle	5.1° - 10°	Medium	5 – 10 km
Moderate	10.1° - 15°	Large	10 – 20 km
Steep	15.1° - 20°	Very large	>20 km
Very steep	>20.1°		

Furthermore, the angle is measured for every ‘breaks of slope’ and it is averaged into degree. The utilized data is the Digital Elevation Model (DEM) from the Shuttle Radar Topography Mission (SRTM) with a resolution of 30m to generate topographic data maps in the form of slopes, slope orientation, and shading relief. At the other hand the radius is measured using averaged value by considering the base volcano shape. At the end, the calculation of 'surface roughness' is applied to the DEM data using the ArcGIS software. Volcanoes were classified into 4 types namely: small flat cones, small step cones, large cones, and massive [4] (Table 2).

Table 2. Classification of volcano’s morphology

Type of volcanoes	Volume	Slope	Elevation
Small flat cones	<6.2 km ³	3-21°	16m - 721m
Small step cones	<9 km ³	14-37°	53 - 971m
Large cones	0.15 km ³ - 178 km ³	3 - 28°	59 – 2.313m
Massive	76-675 km ³	11 - 22°	1.012 – 2.175m

Calculation of surface roughness with root mean square height (RMSH) where n is the number of samples $z(x_i)$ the height value at position x_i and \bar{z} is the mean height. RMSH is calculated along the X/Y profile [16]. Surface Roughness (KP) was obtained from DEM processing with GIS and classified into four categories (Figure 1) [2]. RSMH is calculated with the following equation:

$$RMSH = \sqrt{\frac{1}{n} \sum_{i=1}^n (z(x_i) - \bar{z})^2} \tag{1}$$

In terms of morphology [4], submarine volcanoes are measured from the seafloor with the criteria:

- One.* Nearly circular or elliptical outer sides with positive relief for stratovolcanoes and cones, while maar and caldera volcanoes have mostly negative relief.
- Two.* Characterized by a break of slope that is concave on cones and convex on maars and calderas.
- Three.* Volcanic formations are interpreted based on morphology,

Four. For volcanoes that grew after collapse or erosion, delineated separately from the base of young and older volcanoes.

Classification of volcanoes based on its stages is defined into three types, early stage, long cooling periods, decreasing mafic and increasing felsic minerals, and old volcano [2].

3 Results

3.1 Slope, Radius, and Surface Roughness

DEM analysis consists of slope identification, radius of the volcano, dan calculation of surface roughness, depicted on Figure 1. Slope classes were obtained from DEM data through slope analysis by categorizing them into 5 using natural breaks methods in GIS.

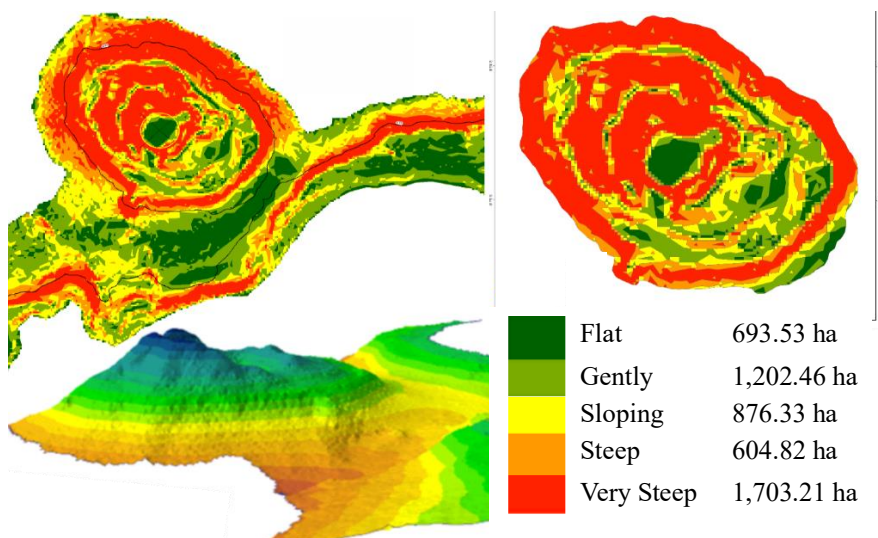


Fig. 1. The slope map of Satonda Volcano, surface roughness map, and 3D view.

Most of the slopes on the Satonda volcano are $5^{\circ} - 10^{\circ}$ (27%) (Table 3). The resulting slope map shows that the northern and northwestern slopes range from steep to very steep, while the southern and southeastern slopes are between $0^{\circ} - 5^{\circ}$ and $5^{\circ} - 10^{\circ}$. In the stratovolcano classification, it is included in Type III, which has an average slope of 9.1° . Volcanic morphology formed in type III is mostly in the form of caldera.

Table 3. Morphometric Characteristics of Satonda volcano

No	Slope			Surface Roughness		
	Slope ($^{\circ}$)	Area (ha)	Percentage	Interval	Area (ha)	Percentage
1	0 – 5	693.53	15.6	0.29 - 15.88	200.75	17.18
2	5 – 10	1,202.46	27.0	15.88 - 31.48	316.30	27.06
3	10 – 15	876.33	19.7	31.48 - 54.80	431.86	36.95
4	15 – 20	604.82	13.6	54.80 - 113.33	219.10	18.75
5	> 20	1,073.21	24.1	113.33 - 134.95	0.67	0.06

Source: Data analysis

The calculation of the average slope is done by making a slope profile of the 8 cardinal directions with each cardinal direction divided according to the break of slope (Table 4). The calculation of the slope resulted that average slope of 18.47°. This slope is close to the average slope of stratovolcano Type I, which is 19.6°.

Table 4. Results of slope measuring

No	Direction	Degree
1	N	24.21°, 20.99°
2	E	19.39°, 13.69°
3	W	18.23°, 22.33°
4	S	16.81°, 6.95°
5	NE	21.02°, 30.72°
6	NW	19.34°, 18.07°
7	SW	19.44 °, 18.07°
8	SE	13.62°, 7.91°

From the cross section, the Satonda volcano is a caldera mountain with mostly steep slopes (Figure 2). The radius of Satonda volcano is close to a circle shape with lengths A-0 2.1 km, B-0 2.9 km, C - 0 1.5 km, and D - 0 1.63 km. The slope shape tends to be convex at the break of slope but concave at the cone or peak where according to [4] is a characteristic of calderas. The Satonda volcano has an average radius of 2.03 km, while Stratovolcano Type I volcanoes have an average radius of 2.1 km.

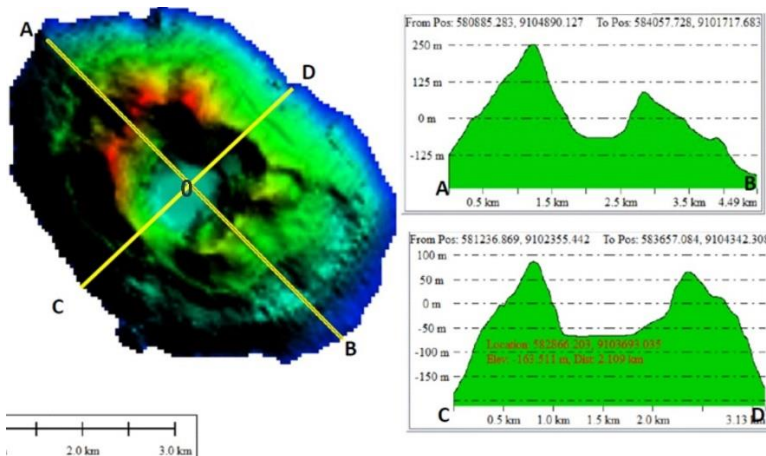


Fig. 2. Cross-section of the Satonda volcano

Surface roughness assessment was obtained from digital DEM processing with spatial analysis and focal statistic techniques. The classification for surface roughness index is grouped into 5 classes with intervals: 1) 0.29 - 15.88, 2) 15.88 - 31.48, 3) 31.48 - 54.80, 4) 54.80 - 113.33, and 5) 113.33 - 134.95 (Table 1). Based on the results of the digital surface roughness assessment, it was found that most (36.95%) of the surface of Mount Satonda has a surface roughness of 31.48 - 54.89 (Figure 3). This value is suitable for a Type II.

3.2 Radial Drainage Pattern

The drainage patterns formed are determined by the inequality of surface slopes and the inequality of rock resistance; the formation of flow patterns can be used as an approach to

understanding geological structures [14]. This type of drainage pattern is found on conical landforms, either volcanoes or dome. Typical radial flow patterns show all stages of volcanic life. In old volcanoes, the flow pattern is getting closer and merges to form a larger flow pattern and even tributary. This is due to the weathering of rocks and the formation of soil layers which are then eroded to form tight valleys. Each river on the volcano will continue to flow straight until it meets the opposite slope which will reverse its flow direction. When two mountains overlap with their respective radial flow patterns, the flow direction will follow the path of the meeting of the two mountains, while young volcanoes will have an almost perfectly round radial flow pattern [6,15]. The drainage pattern is extracted from DEM data into flow direction with GIS. The drainage pattern on the Satonda Island is a radial type. The DEM analyzed is a combination of the DEM of Satonda Island above sea level and bathymetry data measured directly in the field. Drainage patterns on volcanoes in Indonesia are unique because three flow patterns can be found in one geomorphological unit, namely radial, centripetal, and gutter [15]. Gutters are channels or rivers that flow perpendicularly between the radial channels of two intersecting volcanoes. The Satonda volcano is directly adjacent to the Tambora volcano where its foot slopes meet at the bottom of the water and form a gutter (Figure 3).

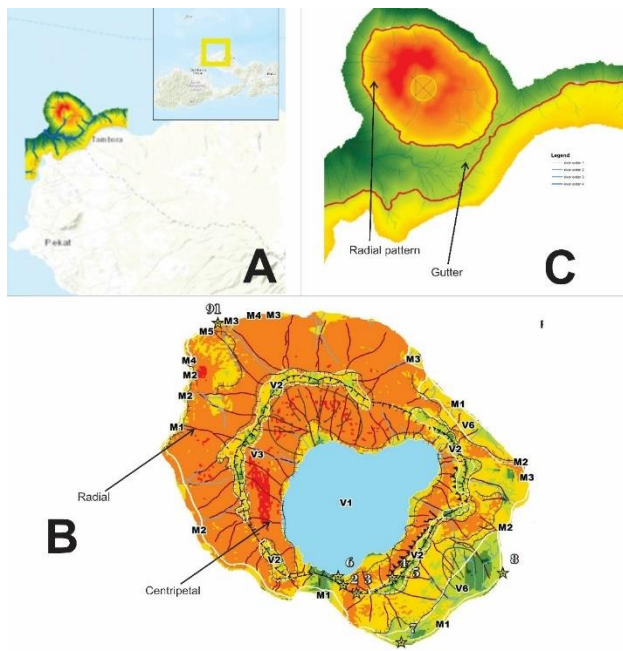


Fig. 3. Morphology of Satonda volcano adjacent to the Tambora volcano (A) where the foot slopes meet and form a Gutter (C), while in the caldera a centripetal flow pattern is formed (B).

3.3 Geological Context

In the Geological Map of Sumbawa, West Nusa Tenggara at a scale of 1: 250,000 published by the Indonesia Geological Agency in 1997, the rocks of Satonda volcano are the same as those of Tambora volcano, namely lava-breccia units with lava, breccia, lava, tuff, and volcanic ash composed of andesite. The rocks are mainly composed of alkaline calcium, and

consist of andesite hornblende and augite-hornblende andesite in the form of pumice and andesite pumice, and andesite augite with biotite. Nangamire pumice at the top of the Young Tambora Volcano (YTV) IV eruption product is a sub Plinian fall deposit consisting of fine-grained lapilli or coarse-grained ash on the western flank of Tambora volcano, as delineated by Takada [16].

4 Discussion

The confluence of Satonda volcano and Tambora volcano forms a gutter. Unlike other gutters, the gutter of Mount Satonda is underwater and was identified through digital processing of drainage patterns. This gutter is considered as the zero point of the height of Satonda volcano, thus the height of Satonda volcano is $200\text{m} + 250\text{m} = 450\text{m}$. However, it should be noted that this understanding of the zero point is only based on the meeting of the volcano's feet while on the other side the depth of the water is unknown because it is not a bathymetric measurement area.

Pyroclastic deposits from the 1815 Tambora eruption show two main eruptive phases, the first producing four tephra fall deposits, while the second formed large pyroclastic flows and waves [17,18]. In addition, the coarsest and most extensive early fallout deposits from the 1815 Tambora eruption were Plinian fallout pumice layers with a thickness of more than 20 cm covering the western flank of Tambora [18]. The Moyo Island and the Satonda Island thickness are more than 10 cm.

Based on the stratigraphic sequence described by Yamamoto [16], it is known that the age of Satonda volcano is between 200,000 - 100,000 years, with the Satonda volcano is being slightly older than the Tambora volcano. However, there are no records of eruption stages like the Tambora volcano. Field observations shows that there is a ridge of fresh light brown lava, while on the southern slope the weathered material is 30 cm thick with pumice. On the slopes of the volcano, lava blocks were found adjacent to the locations of gray-black lapilli and brownish-yellow lapilli. The basaltic-andesite block is a gravitational fall and is found on the southeast and east foothill slopes. On steep rocky coasts, black lava with pyroxene content is found. Following the Isopach map for Nangamire [16] hence the pumice can be found at the Satonda Island (Figure 4).

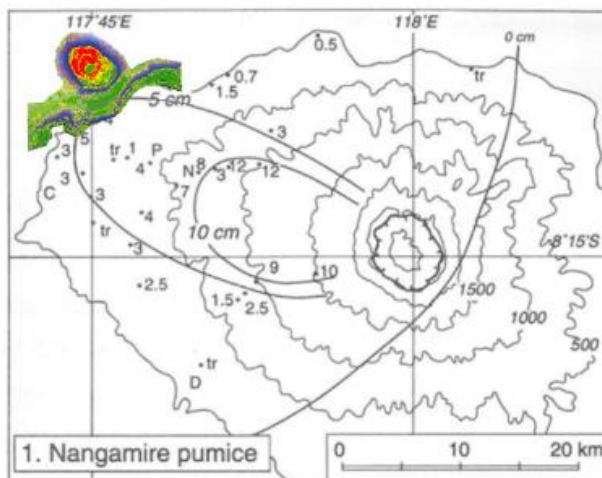


Fig. 4. Isopach map of Nangamire pumice [16] to be extended to the Satonda Island

The overall slope is dominated by 5° - 10° (1,202.46 ha) and $> 20^{\circ}$ (1,073.21 ha). Slopes of 5° - 10° are located on the south and southeast sides of Satonda Island. This is understandable because of the possibility of flank collapses due to lava flows that form a large and sloping backshore. It is land that is most optimally utilized as a tourist attraction. Very steep slopes ($>20^{\circ}$) are on the north and northwest sides with straight slopes in the north and convex in the northwest. In these two parts, the beaches formed are volcanic rock beaches from lava flows and lava block falls.

Based on the slope classification, the Satonda volcano has an average slope of 18.47° including a Type I Stratovolcano but in its development formed a caldera. On the slopes of Satonda Island, there are many lava flows that may have effusive type eruptions. Geologically, a caldera can be formed in two ways: explosion that carries all the material in the cone of the volcano and secondly due to the collapse of the crater wall. However, based on the surface roughness classification, the Satonda volcano is a volcano with high silica content in the magma (Type II). In the volcano development it is found that the caldera formation has an RMSE (surface roughness) of 56.8 with an average slope of 10.7° . The shape of the slope both at the peak (cone) and bounded by the break of slope characterizes the caldera [2]. Stratovolcano reconstruction of Satonda volcano is not easy to do considering that the eruption is thought to have been a one-time event. The evidence when Satonda volcano erupted for one time, hence the type of rocks that make up the slopes of Satonda volcano were found to be dominated by lava rocks and almost no lava. The presence of lapilli and pumice (Nangamire pumice) on the southern slope of Satonda is more associated with pyroclastic fall material from the Tambora volcano. This estimation is reinforced by the estimated direction of the Tambora eruption and the shallowness of the waters between the Satonda Island and the foot slopes of Tambora volcano.

5 Conclusion

The volcano morphometry measurements can be used to trace back volcanic geomorphology processes and used for volcano type classification. The morphometric assessment of the Satonda volcano was carried out on the characteristics of slope, radius, surface roughness, and drainage pattern. Based on the classification done by [2]. The Satonda volcano is classified as Type I and II. Based on the geological map and field survey results, the constituent rocks of the Satonda Island show a dominant uniformity, namely lava rock. The presence of lapilli and pumice on the south side may be the result of pyroclastic fall eruption of the Tambora volcano.

The limited evidence that the Satonda volcano experienced only one eruption and the relatively uniform rock types with a predominance of lava suggest that the Satonda volcano should be considered as a Stratovolcano. Another possibility of the Satonda form is as a Lava Dome. Lava domes are irregular hemispherical formations of volcanic rock mounds, which are formed from lava that is too viscous to flow through the vent that emits it [19]. Usually andesitic to rhyolitic in composition, they can also occur from deadly pyroclastic flows.

The volcano morphometry analysis using the remote sensing and GIS methods can accelerate the volcano classification process, thus this can be utilized for delineation and determining level of danger from volcano eruption. The morphometry analysis for the volcano that emerges from seabed can be applied for delineation of volcano area and for the boundary of volcano morphology to the other geomorphological unit on seabed. Further research is needed on the Satonda volcano regarding its mineral content and stages of volcanic development to answer whether it is a stratovolcano or a lava dome.

Indeed, this study showed that the Satonda Island morphometry analysis can be measured using the high-resolution data through the development of DEM analysis and GIS methods. The bathymetry data on the Satonda Island area captured by a Single Beam Echosounder (SBES) on April 2023 is processed as a Digital Elevation Model (DEM) to measure the hill slope portrayed into 2D shape. The DEM data sourced from the Shuttle Radar Topography Mission (SRTM) with a resolution of 30m is also utilized to generate topographic data maps. Ultimately, the surface roughness calculation is adopted to the DEM using the ArcGIS application.

The surface roughness classification utilized the remote sensing data considering the density value and neighbourhood through the focal statistic tools. The higher resolution of the image (the higher pixel) then the accuracy of surface roughness will be better. This study used the DEM and SRTM data that have higher mean value and standard deviation than ASTER image even though the ASTER resolution is higher. The higher standard deviation range is possible to provide the more accurate performance of morphology characteristics.

This research was organized and funded by Pushidros TNI Al by mean of Expedisi Flores Jalacitra 3. We thank to Pushidros TNI AL for the facilities and to reviewers for meaningful suggestion.

References

- 1 H. T. Verstappen, *The Indones. J. of Geog.*, 27–35 (1994)
- 2 I. Suhendro, Haryono, *Indones. J. Geogr.* **55**(2), 277 (2023)
- 3 A. Tibaldi, *J. Geophys. Res.* **100**(B12), 24521–24535 (1995)
- 4 E. M. Paguican, P. Grosse, G. N. Fabbro, M. Kervyn, *J. Volcanol. Geotherm. Res.* **418**, 107251, (2021)
- 5 A. Jack, “Chandler_et_al-2005-The_Photogrammetric_Record.pdf,” vol. **20**, no. March, pp. 12–26, 2005.
- 6 F. Bretar, M. Arab-Sedze, J. Champion, M. Pierrot-Deseilligny, E. Heggy, S. Jacquemoud, *Remote Sens. Environ.* **135**, 1–11 (2013)
- 7 A. F. M. Hani, D. Sathyamoorthy, V. Sagayan Asirvadam, *Comput. Geosci.* **37**(2), 177–192, (2011)
- 8 J. M. Bennett, *Eng. Opt.* **6**(1), 1–9 (1993)
- 9 A. Rodriguez-Gonzalez, J. L. Fernandez-Turiel, F. J. Perez-Torrado, D. Gimeno, M. Aulinas, *Int. J. Earth Sci.* **99**(3), 645–660 (2010)
- 10 B. W. Mutaqin *et al.*, “Geomorphology of the small island of Tidore and Hiri (North Maluku, Indonesia),” *E3S Web Conf.*, vol. **325**, p. 03012, (2021)
- 11 S. D. Warren, M. G. Hohmann, K. Auerswald, H. Mitasova, vol. **58**, no. 3, pp. 215–233, (2004), doi: 10.1016/j.catena.2004.05.001.
- 12 K. L. A. El-Ashmawy, *Artif. Satell.* **51**(3), 89–97 (2016)
- 13 T. Ullmann, G. Stauch, *Remote Sens.* **12**(19), 1–26 (2020)
- 14 E. R. Zernitz, *J. Geol.* **40**(6), 498–521 (1932)
- 15 C. D. Ollier, J. P. Terry, *Aust. J. Earth Sci.* **46**(4), 515–522 (1999)
- 16 A. B. T. Yamamoto, A. Takada, A. Munandar, N. Kartadinata, *Stratigraphy of the 1815 deposits of Tambora volcano, Indonesia. Report of Research on Volcanic Hazard Assesment in Asia* (International Research and Development Cooperation ITIT Projects, 2000), 80–87
- 17 L. E. A. Brams *et al.*, *Curr. Org. Chem.*, vol. **81**, no. 1, pp. 299–310, (2006), doi: 10.1306/061303740314.
- 18 L. E. A. Brams, *Indones. J. Geosci.*, vol. **1**, no. 1, pp. 49–57, 2006, doi: 10.17014/ijog.vollno1.20066a.
- 19 T. Husain, D. Elsworth, B. Voight, G. Mattioli, P. Jansma, *J. Volcanol. Geotherm. Res.* **285**, 100–117 (2014)